Perturbation and determinacy of nonsmooth systems

Sal Catsis, Cameron L. Hall, Mike R. Jeffrey*

May 9, 2025

Abstract

Take a system where several variables x_i (for $i = 1, 2, ...$) cause decision states h_i to be set independently to values A_i, at any instant, and the outcome then affects how each x_i evolves according to a differential equation. We show here that the probability that the system lies in a given decision state at any instant cannot be determined solely from these differential equations, but is determined by the emergence of a dynamical attractor. Moreover this attractor is sensitive to small perturbations in *how* the decisions are enacted, and even how the system's evolution is calculated. If the probability that x_1 decides 'A_1' is $P(A_1)$ and x_2 decides 'A_2' is $P(A_2)$, for instance, the probability that x_1 decides 'A_1' and x_2 decides 'A_2' at any moment is not generally $P(A_1)P(A_2)$, despite the independence of their decisions (nor is it any other determinable quantity such as $P(A_1)P(A_2|A_1)$). Only certain weighted sums of probabilities of being in different decision states are determined by the logic of the system.

This result comes from formulating this simple decision-making scenario as a dynamical system with discontinuities (or *piecewise-smooth* or *nonsmooth* system), and exposes a need to better understand the indeterminacy of discontinuous models, and how they behave under perturbation. The perturbations of interest might represent physical properties neglected in an idealised model with discontinuities, or imperfections introduced in simulations, perhaps by discretising the system, by smoothing out a discontinuity, or delaying a discontinuity's effect on the system.

We define concepts here that permit us to characterise the determinacy of discontinuous systems and compare them under such perturbations. We find that although the overall dynamics of a system is indeterminable at a discontinuity, certain measures of occupancy either side of a discontinuity *are* determinable. These give a refined insight into Filippov's differential inclusions, and give more precision to Utkin's notion of *equivalent* dynamics, interestingly allowing us to treat discontinuities in dynamical systems similarly to Markov processes.

*School of Eng Mathematics, University of Bristol, Ada Lovelace Building, Bristol BS8 1TW, UK, email: mike.jeffrey@bristol.ac.uk

Contents

1 Introduction

Consider a dynamical system $\dot{\mathbf{x}} = \mathbf{f}(\mathbf{x})$ that switches between different modes of behaviour as $\mathbf{x}$ moves between open domains R_i, say as

$$\dot{\mathbf{x}} = \mathbf{f}_i(\mathbf{x}) \quad \text{for} \quad \mathbf{x} \in R_i \tag{1}$$

for some $i = 0, 1, 2, ..., d$. Clearly the solutions $\mathbf{x}(t)$ of these systems are ill-defined at the boundaries of the regions R_i. To obtain solutions at these boundaries, we must add further rules or assumptions about the dynamics there, e.g. smoothing out any jumps in (1) at the boundaries, or defining a 'Filippov system' at the boundaries (from [16]). When we do this, to what extent can we consider such models to be approximated by the system (1)?

The importance of these ideas is that models like this have become widespread in applications, and there are numerous methods and theory to obtain their qualitative dynamics. Figure 1 summarises something of the scope of contexts where such models arise, and the varied means of

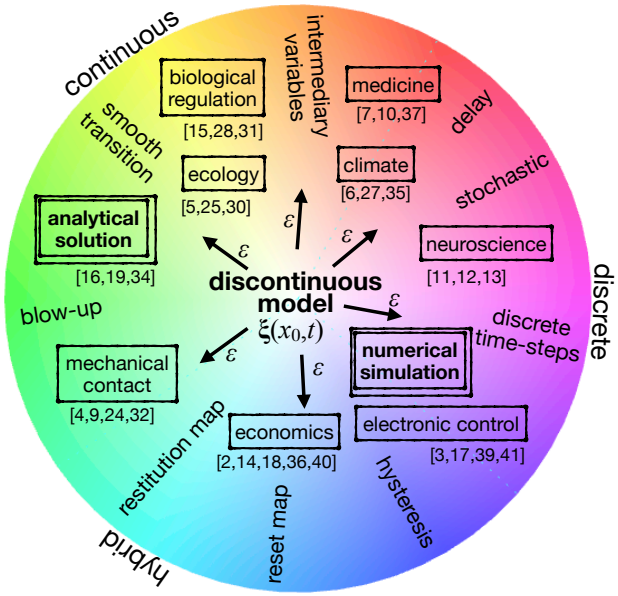

Figure 1: The applied landscape of applications modelled as dynamical systems with discontinuities. This is not exhaustive, but a few representative and recent citations are given, with an indication of the *perturbations* of the discontinuity involved in either the modelled system (e.g. delay, stochasticity, hysteresis, intermediary variables), or the method of analysis (e.g. smoothing, blow-up, or time discretisation).

analysing them. A sample of recent or notable references are given in the figure. It is not our aim to survey these here, and these references are merely a glimpse into the ways that systems of the form (1) are used to model abrupt changes of behaviour that occur in genetics, in neuron firing, in medicine, in economics, in mechanics, in electronics, in climatology, and elsewhere. Depending on the context, such switches may actually be smooth, they may involve delays, hysteresis, or occur via a reset (e.g. impact) map. There are a range of numerical and analytic methods used to simulate them, by introducing blow-up coordinates or intermediary variables, by smoothing out the discontinuity, or discretising.

To illustrate our results throughout this paper we will use a simple two-player thought experiment, the *pilots' dilemma* scenario from [21], in which two pilots attempt to steer a spacecraft along a desired path, as a simple prototype of a two-switch system inspired particularly by models of regulation in genetics, electronics, and economics.

Central to our problem is the question: what kinds of system does (1) approximate, and conversely, what equations or simulations approximate the model (1)? How are we mathematically justified in considering (1), lying at the centre of fig. 1, as lying ε-close to any of the systems surrounding it in some space of ε-perturbations? The answers to these questions are not clear, precisely because (1) is ill-defined at the discontinuity between regions R_i. Yet systems like this are used widely and routinely in modern mathematical modelling, to represent switching or other abrupt changes. We will show the ambiguity here of using discontinuities as approximations, and define concepts to refine our understanding of them.

To handle the ill-definedness at a discontinuity with more generality than previous works, we propose to distinguish between:

1. the constitutive laws of a model in the idealised form (1), whose solutions are ill-defined at the discontinuities, and

2. the 'equivalent' dynamics of any system that tends to (1) in some limit, which we will define here.

To do this, let us assume there exists some trajectory $\mathbf{x}(t) = \boldsymbol{\xi}(\mathbf{x}_0, t) \in \mathbb{R}^n$ of (1) with $\boldsymbol{\xi}(\mathbf{x}_0, 0) = \mathbf{x}_0$, and consider a perturbation of this, some $\boldsymbol{\xi}(\mathbf{x}_0, t, \varepsilon)$, for small $\varepsilon \geq 0$ such that

$$\lim_{\varepsilon \to 0} \boldsymbol{\xi}(\mathbf{x}_0, t, \varepsilon) = \boldsymbol{\xi}(\mathbf{x}_0, t) \ . \tag{2}$$

The function $\boldsymbol{\xi}(\mathbf{x}_0, t, \varepsilon)$ might represent a physical system that is supposed to be modelled by $\boldsymbol{\xi}(\mathbf{x}_0, t)$, or it could represent any analytical or numerical

simulation of $\boldsymbol{\xi}(\mathbf{x}_0, t)$, i.e. any system in fig. 1 as a perturbation of $\boldsymbol{\xi}(\mathbf{x}_0, t)$ at the centre.

Now, within the open domains R_i, the limit of $(\boldsymbol{\xi}(T, \mathbf{x}_0) - \mathbf{x}_0)/\delta t$ exists as $\delta t \to 0$, and we can write that (1) holds with

$$\mathbf{f}_i(\mathbf{x}) := \lim_{\delta t \to 0} \frac{\boldsymbol{\xi}(t + \delta t, \mathbf{x}) - \boldsymbol{\xi}(t, \mathbf{x})}{\delta t} \ . \tag{3}$$

At the boundaries of any R_i, however, $(\boldsymbol{\xi}(t + \delta t, \mathbf{x}) - \boldsymbol{\xi}(t, \mathbf{x}))/\delta t$ does not have a well-defined limit, leaving $\dot{\mathbf{x}}$ undefined. Rather than seeking to alter this fact by placing further assumptions on (1), let us consider any additional assumptions to be strictly part of the ε-perturbed system with trajectory $\boldsymbol{\xi}(T, \mathbf{x}_0, \varepsilon)$, and assume that $(\boldsymbol{\xi}(t + \delta t, \mathbf{x}; \varepsilon) - \boldsymbol{\xi}(t, \mathbf{x}; \varepsilon))/\delta t$ does have a well-defined limit. We then use this to define an *equivalent* motion to (1) as

$$\langle \dot{\mathbf{x}} \rangle = \lim_{\delta t \to 0} \lim_{\varepsilon \to 0} \frac{\boldsymbol{\xi}(t + \delta t, \mathbf{x}; \varepsilon) - \boldsymbol{\xi}(t, \mathbf{x}; \varepsilon)}{\delta t} \ . \tag{4}$$

We will propose below that, to understand the perturbation of a system at a discontinuity, it is vital to distinguish clearly between the *instantaneous motion* (1), which satisfies (3) only inside the regions R_i, and the *equivalent motion* (4) which holds everywhere. By carefully making this distinction, we can resolve possible indeterminacies that Filippov brought to light already in [16], and derive useful quantities for measuring how the dynamics at a discontinuity varies under perturbation.

To characterise this equivalent dynamics we will introduce a function μ_i that measures the probability that a trajectory $\boldsymbol{\xi}(T, \mathbf{x}, \varepsilon)$ is in the mode $\mathbf{f}_i$ at any instant. Then, associated with μ_i, there exists a *switching probability matrix* $\underline{\underline{P}}$ with elements P_{ki}, giving the probability that the trajectory is switching from mode vector $\mathbf{f}_k$ to $\mathbf{f}_i$ at any instant, with the properties that the rows of $\underline{\underline{P}}$ sum to unity, and $\boldsymbol{\mu} = (\mu_1, ..., \mu_d)^{\mathsf{Tr}}$ is the eigenvector of its transpose, that is $\underline{\underline{P}}^{\mathsf{Tr}} \boldsymbol{\mu} = \boldsymbol{\mu}$, or

$$\sum_i P_{ki} = 1 \ , \qquad \sum_k P_{ki} \mu_k = \mu_i \ . \tag{5}$$

This allows us to view the transitions between modes $k \mapsto i$ similarly to a Markov process with transition matrix $\underline{\underline{P}}$. The identification with Markov processes becomes exact if the functions $\boldsymbol{\xi}(T, \mathbf{x}_0, \varepsilon)$ depend only on the present time t (i.e. not on previous times), and if the switching between modes is stochastic. It was shown in [8] that even deterministic simulations of a system like (1), and even with only two modes, result in mode switching

that is so surprisingly complex that in simulations it may appear empirically as if it is stochastic. These quantities μ_i and P_{ki} were used as numerical tools in [8], and we refine and generalise their definitions here.

When a system evolves along a discontinuity, known as *sliding*, we will show that the probabilities μ_i are not-uniquely defined by the $\varepsilon = 0$ discontinuous system (1), but that there do exist certain sums of the μ_is, weighted by the modes $\mathbf{f}_i$, that *are* well-defined.

These do not appear to have come to light in previous literature on discontinuous systems, and they allow us to show a counterintuitive feature of discontinuous systems not revealed before: that logical behaviours encoded into their equations of motion do not hold over long times. Let the mode $\mathbf{f}_0$ in (1) be selected when two logical indicators, some h_1 and h_2 that take values 0 or 1, are both set to 0. As the system evolves, let the observed probability that $h_j = 1$ at any time be some $P(h_j = 1)$. Does the probability that the system lies in this mode, $P(h_1 = 1 \ \wedge \ h_2 = 1)$, obey

$$P(h_1 = 1 \ \wedge \ h_2 = 1) \ = \ P(h_1 = 1)P(h_2 = 1) \ , \tag{6}$$

or perhaps its conditional form $P(h_1 = 1 \ \wedge \ h_2 = 1) \ = \ P(h_1 = 1)P(h_2 = 1 \mid h_1 = 1)$? We will show that no such relations hold generally, regardless of how independently the two indicators h_j are chosen. Moreover, the values of probabilities like $P(h_1 = 1)$, $P(h_2 = 1)$, and $P(h_1 = 1 \ \wedge \ h_2 = 1)$, are highly dependent on the method of simulation (i.e. the perturbation of (1)), leading to markedly different outcomes of their dynamics.

We will show that simulations obtained by smoothing out the discontinuity, which correspond here to replacing the h_j with smooth transitions between 0 and 1, are a special case in which (6) does hold, but this will then break down if the system is otherwise perturbed, e.g. discretised for the purposes of numerical modelling or measurement, or when switching between values of each h_j involve delays.

The paper is set out as follows. In section 2 we describe the two-player game of the pilots' dilemma, simulating three variants of the game that we will use to illustrate our results later. Section 3 introduces our definition of *equivalent dynamics*, with the accompanying probabilities of mode occupancy μ_i and switching probability P_{ki} in section 3.1-section 3.2. Generally these μ_i and P_{ki} are not well-determined by the logical structure (differential equations) of a system, but we then derive in section 3.3 certain μ-sums that *are* well-determined. Section 4 demonstrates these results using the decision scenario from fig. 2, and some closing remarks are made in section 5.

For both theorists and users of nonsmooth models, some of the concepts here will seem familiar, such as the existence of certain coefficients μ_i and

λ_j useful in expressing a discontinuous system (1) as either a convex hull or a convex canopy. That these are familiar is a tribute to the insight of the works of A. F. Filippov and V. I. Utkin where these concepts seem to have first appeared, e.g. [16, 38]. In this work we refine and generalise these concepts substantially, defining them as integrals over the motion, and instigating, we hope, a new and more robust paradigm in the understanding of nonsmooth dynamical systems, both as applied models, and perhaps provoking the development of a more extensive perturbation theory.

2 Illustration: a two-player decision game

Consider a spacecraft controlled by two pilots, one controlling its yaw rate, x_1, the other controlling its pitch rate, x_2, by firing a yaw and pitch thruster, respectively, in an attempt to control their craft onto a steady heading $x_1 \approx x_2 \approx 0$. Each thrust also affects their forward speed, y. The scenario was set out in [21] as a thought experiment to explore the relationship between discontinuous systems and decision making. Here we take a particularly simple form that helps explore the unpredictability of such a system under different perturbations.

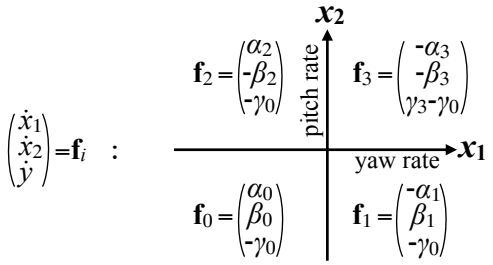

Figure 2: A set of accelerations for the pilots' scenario in the four thruster modes $i = 0, 1, 2, 3$, corresponding to thrusting right-up (0), left-up (1), right-down (2), left-down (3), and in terms of indicators $h_1 h_2$ we will write these as switch states $00, 10, 01, 11$. These give equations of motion $(\dot{x}_1, \dot{x}_2, \dot{y})^{\mathsf{Tr}} = \mathbf{f}_i$. For simplicity here we assume a constant retardation $\dot{y} = -\gamma_0$, except for an additional acceleration γ_3 felt in mode '3', and all parameters $\alpha_i, \beta_i, \gamma_i$, are taken to be constant and non-negative.

The spacecraft's equation of motion is then $(\dot{x}_1, \dot{x}_2, \dot{y}) = \mathbf{f}_i$, of the form (1) with $\mathbf{f}_i$ taking one of the four modes in fig. 2. The four quadrants of the (x_1, x_2) plane form the four regions R_1, R_2, R_3, R_4.

We will take all of the parameters as positive, so that the pilots control the system onto a forward heading $x_1 = x_2 = 0$.

We begin by simulating this system using a number of different methods ①-⑦ (described briefly below and more completely in appendix A), which reveal surprising unpredictability in the ship's motion depending on fine details of each method. We then set out to explain and quantify this unpredictability in the remainder of the paper. In fig. 3(i-iii) we simulate three different variants of the pilots' scenario, each with different parameters as given in the caption, and whose significance we describe later.

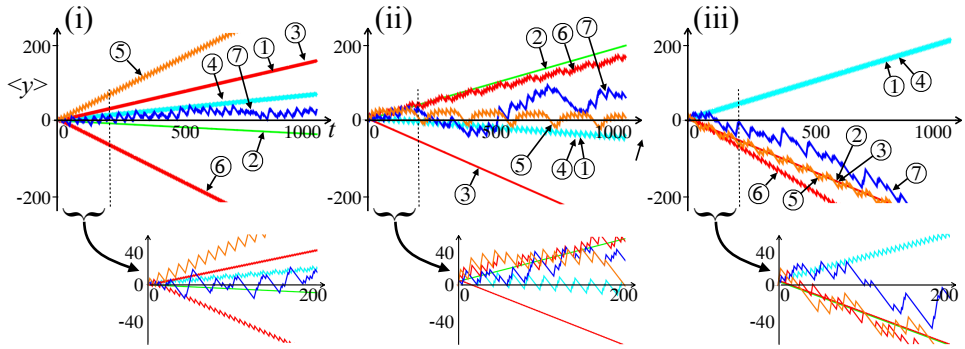

Figure 3: Simulations of the two-pilot scenario from fig. 2. Three different variants of the system (i)-(iii) are shown. Each variant is simulated using different methods ①-⑦ that all approximate (1), so why do different simulations within the same game show conflicting outcomes? Each is shown over time $t \in [0, 1000]$, with the interval $t \in [0, 200]$ magnified below. The different simulations are explained in appendix A: ① discrete time, ② smoothed, ③ smoothed in discrete time, ④ shallower sigmoid in discrete time, ⑤ intermediary variable, ⑥ delay, ⑦ random delay. The parameter values for the three variants are:
(i) $\alpha_0 = 2, \beta_0 = 2, \alpha_1 = 1, \beta_1 = 2, \alpha_2 = 3, \beta_2 = 1, \alpha_3 = 3, \beta_3 = 4, \gamma_0 = 1, \gamma_3 = 4,$
(ii) $\alpha_0 = 1, \beta_0 = 3, \alpha_1 = 2, \beta_1 = 2, \alpha_2 = 2, \beta_2 = 3, \alpha_3 = 1, \beta_3 = 4, \gamma_0 = 1, \gamma_3 = 6,$
(iii) $\alpha_0 = 3, \beta_0 = 1, \alpha_1 = 2, \beta_1 = 1, \alpha_2 = 3, \beta_2 = 4, \alpha_3 = 2, \beta_3 = 4, \gamma_0 = 1, \gamma_3 = 6.$

For each variant (i)-(iii), each simulation method ①-⑦ is a perturbation of the idealised discontinuous system (1), that is, tending to (1) in some limit $\varepsilon \to 0$, with the modes $\mathbf{f}_i$ given in fig. 2. Despite each method constituting a small perturbation of (1), their outcomes differ markedly within each scenario (i)-(iii). Note also that sensitivity to these perturbations occurs in all three variants (i)-(iii).

The methods are described in appendix A as their details are not essential, and others could be considered, but let us summarise them briefly. We encourage the reader to consider how they might simulate such a system, or how they might approach a similar scenario in applications of their own interest. In ① the discontinuity is smoothed out by replacing each h_j with

a sigmoid function transitioning between 0 and 1 over a layer $|x_j| \leq \varepsilon$. In ② − ⑦ the simulation takes a simple discretisation $\mathbf{x} \mapsto \mathbf{x} + \Delta t\ \mathbf{f}_i$ with time-step $\Delta t = \varepsilon$, and then introduces either small delays, stochasticity, or intermediary variables in the pilots' decision process. Note that since the $\mathbf{f}_i$ are constants, we can re-scale $\mathbf{x} = \varepsilon\mathbf{x}'$ to give $\mathbf{x}' \mapsto \mathbf{x}' + \mathbf{f}_i$, so in our simulations we set $\Delta t = 1$, but the results remain unchanged by taking $\Delta t = \varepsilon$ to be arbitrarily small. Hence these results remain unchanged by taking $\varepsilon \to 0$, in which limit we obtain exactly the model (1) (with the respective modes given in fig. 3).

This kind of unpredictability has been noted in previous works, e.g. [20, 21]. The importance of (i)-(iii) is that the seminal ideas of Filippov and Utkin [16, 39] imply unpredictability in (i), but not in (ii)-(iii), which they would seem to imply are fully determined and hence predictable (these differences are explained more in section 4). This implication followed from the Filippov's set-valued inclusion uniquely determining the motion in the case of (ii-iii), due to some dependence between the modes $\mathbf{f}_i$, but not in (i) (for detailed discussion see any of [16, 19, 20, 21]). Here this means that (ii) and (iii) should each show a single curve with only small perturbations. These ideas were propagated as recently as [23] by Utkin himself and one of the present authors. Here we will dispel these myths, and provide the quantities needed to study such unpredictability with rigour.

We note that there are some agreements between simulation methods in fig. 3, as one or other curve may coincide, though with no obvious pattern, and always susceptible to change subject to small changes in parameters of the simulation. The point is that so many simulations are able to *dis*agree, and what determines whether two simulations will agree is unclear. If we are to understand the reliability of any such simulations of nonsmooth systems, we need closer insight into why such variability is permitted.

Note importantly that we are careful to label the simulated value of y as the equivalent value $\langle y \rangle$, as it cannot be considered a property of the idealised system (1), clearly, since each of the simulations disagree, instead they constitute different *singular* perturbations $\boldsymbol{\xi}(\mathbf{x}_0, t, \varepsilon)$ of the limiting solution $\boldsymbol{\xi}(\mathbf{x}_0, t)$ of (1); singular because they disagree in the limit $\varepsilon \to 0$.

3 Equivalent motion and switching probabilities

In a differentiable system, the righthand side of the equation $\dot{\mathbf{x}} = \mathbf{f}(\mathbf{x})$ governs behaviour at all times, and so the dynamics of the system is given by its first integral. In a system of the form (1), of course, this fails, as the

righthand side ceases to be well-defined at the discontinuity, but similar to generalised functions, we can still consider the first integral as being meaningful. As we explore here, this in effect means considering solutions over intervals of time $t \in [0, T]$, rather than at a time instant t, and representing this motion in terms of integral quantities. When we consider the limit $T \to 0$, we obtain equations of *equivalent motion* over these intervals.

To obtain this we introduce the following.

Definition 3.1. The *equivalent motion* associated with the nonsmooth system (1) is given by

$$\langle \dot{\mathbf{x}} \rangle = \lim_{T \to 0} \lim_{\varepsilon \to 0} \frac{\boldsymbol{\xi}(t+T, \mathbf{x}, \varepsilon) - \boldsymbol{\xi}(t, \mathbf{x}, \varepsilon)}{T} \tag{7}$$

$$\text{where} \qquad \boldsymbol{\xi}(T, \mathbf{x}_0, \varepsilon) = \mathbf{x}_0 + \int_0^T dt\, \mathbf{f}(\mathbf{x}(t); \varepsilon) \ ,$$

$$\text{and} \qquad \lim_{\varepsilon \to 0} \mathbf{f}(\mathbf{x}; \varepsilon) = \mathbf{f}_i(\mathbf{x}) \quad \text{for } \ \mathbf{x} \in R_i \ ,$$

for some real $T \geq 0$ and $\varepsilon \geq 0$ and initial point $\mathbf{x}_0$, with $f(\mathbf{x}(t); \varepsilon)$ defined such that the limit $\langle \dot{\mathbf{x}} \rangle$ exists, and $\boldsymbol{\xi}(T, \mathbf{x}_0, \varepsilon)$ at any moment T lies in any one of the mode regions R_i for $i = 1, ..., d$.

We will not make any further specification of $\mathbf{f}(\mathbf{x}; \varepsilon)$ other than that it limits to the modes $\mathbf{f}_i(\mathbf{x})$ on the open regions R_i (they may take any of the rich forms of perturbation in fig. 1 or fig. 3 and more). Without further knowledge of either $\mathbf{f}(\mathbf{x}; \varepsilon)$ or $\boldsymbol{\xi}(T, \mathbf{x}_0, \varepsilon)$, we can write an expression for $\langle \dot{\mathbf{x}} \rangle$ as a convex hull of the modes $\mathbf{f}_i$ in the neighbourhood of a point $\mathbf{x}$. In the time interval $[0, T]$, say the state $\mathbf{x}(t)$ spends some proportion of time μ_i in each mode $\mathbf{f}_i$, then its equivalent motion is given by

$$\langle \dot{\mathbf{x}} \rangle = \sum_{i=0,...,d} \mu_i \mathbf{f}_i(\mathbf{x}) \ , \tag{8}$$

such that

$$\sum_{i=0,...,d} \mu_i = 1 \ . \tag{9}$$

For $\mathbf{x} \in R_i$, for example, we would have that $\mu_i = 1$ and all other $\mu_{k \neq i} = 0$. If $\mathbf{x}$ lies on the boundary of some R_i, then μ_i will lie between 0 and 1.

The righthand side of (8) has been seen many times in nonsmooth systems, e.g. in [16, 1, 23]. The first important point here is that it appears

not as an expression of the instantaneous motion $\dot{\mathbf{x}}$, but strictly of the *equivalent motion* $\langle\dot{\mathbf{x}}\rangle$. The second important point is that, rather than merely thinking of the μ_i as coefficients of the convex hull in (8), we will now give these a more precise definition that allows us to derive their values for any perturbation $\mathbf{f}(\mathbf{x};\varepsilon)$ of the righthand side of (1).

We will then show in section 3 that the μ_is in general cannot be uniquely determined from the discontinuous system, but there exists a family of 'μ sums' that *are* well-defined, and which express weighted probabilities of the mode the system occupies at any instant.

Along with defining the *mode occupancies* μ_i, we define an associated *switching probability* P_{ki} from mode k to i, necessary to understand the system's sensitivity to perturbation. We define these over a time interval $[0,T]$ and prove certain basic properties. An augmented form for $T\to\infty$ characterises the equivalent *asymptotic* dynamics of an attractor.

As evident from fig. 3, systems with discontinuities can behave very differently depending on whether they evolve in a continuous or discrete manner. Hence we define μ and P both in continuous time and in discontinuous time.

We will make use of a *mode indicator* that detects which region the system is in at a given point,

$$m_i(\mathbf{x}) = \begin{cases} 1 & \text{if } \mathbf{x}\in R_i\ , \\ 0 & \text{if } \mathbf{x}\notin \overline{R}_i\ , \end{cases} \tag{10a}$$

for $i=0,1,...,d$, where $\overline{R}_i$ denotes the closure of R_i. We let $m_i\in[0,1]$ if $\mathbf{x}\in\partial R_i$ (lies on a boundary of any region R_i), such that

$$\sum_{i=0,1,...,d} m_i(\mathbf{x}) = 1 \qquad \text{for all } \mathbf{x}\ . \tag{10b}$$

An alternative form of (1) occurs commonly in biological, mechanical, and electronic applications, where a system depends on *switch indicators*

$$h_j(\mathbf{x}) = \text{step}(\sigma_j(\mathbf{x}))\ , \tag{11}$$

for $j=1,...,r$, and for some smooth functions $\sigma_j:\mathbb{R}^n\to\mathbb{R}$, where step$(s)$ denotes the Heaviside step function with value 0 if $s<0$ and 1 if $s>0$. In terms of these, the modes $\mathbf{f}_i$ in (1) can be written as

$$\mathbf{f}_i(\mathbf{x}) = \mathbf{f}(\mathbf{x};h_1,...,h_r) \quad \text{with} \quad i=\mathcal{B}(h_1,...,h_r)\ , \tag{12}$$

where $i = \mathcal{B}(h_1, ..., h_r)$ represents some one-to-one correspondence between the switch indicators h_j and the indices i (or between the orthants $x_j \gtrless 0$ and the regions R_i). The general form of (12) is the '*convex canopy*' defined in [19]. We will see an example of this in section 4.

The switch indicators h_j are termed 'switching multipliers' in [19] or discontinuous 'controls' (leading to 'equivalent controls') in [16, 38], but we will refine both these notions here.

Below we will associate the indices j and i strictly with the different indicators h_j and m_i, respectively, and will define corresponding probabilities λ_j and μ_i, summarised here for ease of reference:

index		indicator		probability
$j \in \{1, ..., r\}$	$\rightarrow$	h_j	$\rightarrow$	λ_j
$i \in \{0, ..., d\}$	$\rightarrow$	m_i	$\rightarrow$	μ_i

the *indicator* pertaining to *instantaneous* dynamics, the *probability* pertaining to *equivalent* dynamics.

3.1 In continuous time

Let us define the proportion of time μ_i that a trajectory spends in the mode i, the proportion of time P_{ki} in which the mode switches from k to i, and the proportion of time λ_j that a trajectory lies in any mode with $h_j = 1$, as follows.

Definition 3.2. Given a system (1) with indicator functions (10) and (11), for some $T, \Delta T \geq 0$, define

$$\lambda_j(T) = \frac{1}{T} \int_0^T dt\ h_j(\mathbf{x}(t)) \ , \tag{13}$$

$$\mu_i(T) = \frac{1}{T} \int_0^T dt\ m_i(\mathbf{x}(t)) \ , \tag{14}$$

$$P_{ki}(T) = \frac{1}{\mu_k T} \lim_{\Delta t \to 0} \int_0^T dt\ m_k(\mathbf{x}(t)) m_i(\mathbf{x}(t + \Delta t)) \ , \tag{15}$$

where $j \in \{1, ..., r\}$ and $k, i \in \{0, ..., d\}$. We will call λ_j the *switching multiplier*, μ_i the *mode occupancy*, P_{ki} the *switching probability* from mode k to i.

So if we define a solution trajectory $\Gamma_{\mathbf{x}_0} = \{\mathbf{x}(t) \ : \ t \in [0, T],\ \mathbf{x}(0) = \mathbf{x}_0\}$, such that $\dot{\mathbf{x}}(t) = \mathbf{f}_i(\mathbf{x})$ for $\mathbf{x}(t) \in R_i$, then μ_i gives the proportion of time

on $\Gamma_{\mathbf{x}_0}$ for which $\mathbf{x}(t)$ is evolving in the mode i, i.e. for which $m_i(\mathbf{x}(t)) = 1$, while P_{ki} gives the probability that the mode is changing from k to i at any time $t \in [0, T]$ along the trajectory $\Gamma_{\mathbf{x}_0}$. Similarly λ_j gives the proportion of time on $\Gamma_{\mathbf{x}_0}$ that $\mathbf{x}(t)$ is in the group of modes satisfying $h_j(\mathbf{x}(t)) = 1$.

The matrix $\underline{\underline{P}}$ has two key properties that identify it as the switching probability matrix between the modes $\mathbf{f}_i$, and which it shares with the transition matrix of a Markov process (see e.g. [29, 26]).

Lemma 3.1. The column vector $\mu = (\mu_1, ..., \mu_{2^r})^{\mathsf{Tr}}$ is the right eigenvector of $\underline{\underline{P}}^{\mathsf{Tr}}$, that is, $\underline{\underline{P}}^{\mathsf{Tr}}\boldsymbol{\mu} = \boldsymbol{\mu}$ or

$$\sum_{k=0,1,...,d} P_{ki}\mu_k = \mu_i \ .$$

Proof. By direct calculation, exchanging the order of the sum and the integral, using the fact that the sum over all m_k is unity,

$$\begin{aligned}
\sum_{k=0,1,...,d} P_{ki}\mu_k &= \sum_k \frac{1}{T} \lim_{\Delta t\to 0} \int_0^T dt\ m_k(\mathbf{x}(t)) m_i(\mathbf{x}(t+\Delta t)) \\
&= \frac{1}{T} \lim_{\Delta t\to 0} \int_0^T dt\ \left(\sum_k m_k(\mathbf{x}(t))\right) m_i(\mathbf{x}(t+\Delta t)) \\
&= \frac{1}{T} \lim_{\Delta t\to 0} \int_0^T dt\ m_i(\mathbf{x}(t+\Delta t)) \\
&= \frac{1}{T} \int_0^T dt\ m_i(\mathbf{x}(t)) \quad = \quad \mu_i \ . \qquad (16)
\end{aligned}$$

□

Lemma 3.2. The rows of $\underline{\underline{P}}$ sum to unity.

Proof. Again this is a simple calculation, exchanging the order of the sum and the integral, and using the fact that the sum over all m_i is unity,

$$\begin{aligned}
\sum_i P_{ki} &= \frac{1}{\mu_k T} \sum_i \lim_{\Delta t\to 0} \int_0^T dt\ m_k(\mathbf{x}(t)) m_i(\mathbf{x}(t+\Delta t)) \\
&= \frac{1}{\mu_k T} \lim_{\Delta t\to 0} \int_0^T dt\ m_k(\mathbf{x}(t)) \left(\sum_i m_i(\mathbf{x}(t+\Delta t))\right) \\
&= \frac{1}{\mu_k T} \lim_{\Delta t\to 0} \int_0^T dt\ m_k(\mathbf{x}(t)) \quad = \quad \frac{1}{\mu_k}\mu_k \quad = \quad 1 \ . \qquad (17)
\end{aligned}$$

□

Since λ_j gives the proportion of time for which $h_j(\mathbf{x}(t)) > 0$, and μ_i gives the proportion of time for which $m_i(\mathbf{x}(t)) > 0$, with i and j related by some $i = \mathcal{B}(h_1, ..., h_r)$ from (12), we must have the following.

Lemma 3.3. The switching mulipliers λ_j are sums of the mode occupancies μ_i for which $i = \mathcal{B}(h_1, ..., h_r)$, with $h_j = 1$ and all other $h_{k\neq j} \in \{0, 1\}$, or

$$\lambda_j \;=\; \sum_{i \in L_j} \mu_i \tag{18}$$

where

$$L_j = \left\{ i \in \{0, d_r\} \;:\; \begin{array}{l} i = \mathcal{B}(h_1, ..., h_r) \\ h_j = 1,\; h_{j\neq k} \in \{0, 1\} \end{array} \right\} .$$

Proof. By direct calculation, exchanging the order of the sum and the integral, then using the fact that L_j contains all mode indices i for which $h_j = 1$,

$$\begin{aligned} \sum_{i \in L_j} \mu_i &= \sum_{i \in L_j} \frac{1}{T} \int_0^T dt\; m_i(\mathbf{x}(t)) \\ &= \frac{1}{T} \int_0^T dt\; \sum_{i \in L_j} m_i(\mathbf{x}(t)) \\ &= \frac{1}{T} \int_0^T dt\; h_j\left(\mathbf{x}\right) \;=\; \lambda_j \; . \end{aligned} \tag{19}$$

□

An augmented form of μ_i, P_{ki} and λ_j, will be of use for characterising attractors.

Definition 3.3. Given a system (1) with indicator function (10), define the *asymptotic switching multiplier* $\overline{\lambda}_j$, the *asymptotic mode occupancy* $\overline{\mu}_i$, and the *asymptotic switching probability* $\overline{P}_{ki}$ from mode k to i, by

$$\overline{\lambda}_j = \lim_{T\to\infty} \frac{1}{T} \int_0^\infty dt\; e^{-t/T} h_j(\mathbf{x}(t)) \; , \tag{20}$$

$$\overline{\mu}_i = \lim_{T\to\infty} \frac{1}{T} \int_0^\infty dt\; e^{-t/T} m_i(\mathbf{x}(t)) \; , \tag{21}$$

$$\overline{P}_{ki} = \frac{1}{\mu_k} \lim_{T\to\infty} \lim_{\Delta t\to 0} \frac{1}{T} \int_0^\infty dt\; e^{-t/T} m_k(\mathbf{x}(t)) m_i(\mathbf{x}(t + \Delta t)) \; , \tag{22}$$

where $j \in \{1, ..., r\}$ and $k, i \in \{0, ..., d\}$.

We will sometimes drop the term 'asymptotic' when it is clear we are discussing an attractor.

Typically these limits will exist only for solutions that tend to an attractor. They allow us to measure how much time the system spends in a mode i, or switching between modes k to i, when on an attractor. In practice, to calculate $\overline{\mu}_i$ and $\overline{P}_i$, one need only take T large enough that their integrals/sums converge onto steady values.

3.2 In discrete time

The system (1) is expressed as varying in continuous time, but of course many models or simulations evolve in discrete time-steps. So let us consider the discrete time analogue of (1),

$$\mathbf{x}_{n+1} = \mathbf{x}_n + \Delta t(\mathbf{x}_n)\mathbf{f}_i(\mathbf{x}_n) + \mathcal{O}\left(\Delta t^2(\mathbf{x}_n)\right) \quad \text{for } \mathbf{x}_n \in R_i \ . \tag{23}$$

Of course, *any* computational simulation necessarily makes use of some kind of discretisation.

The definitions of equivalent motion, and of μ_i, P_{ki}, λ_j, for a system evolving in discrete time-steps are then as follows.

Definition 3.4. The *equivalent motion* associated with the nonsmooth system (23) is given by

$$\langle \dot{\mathbf{x}} \rangle = \lim_{T\to 0} \lim_{\varepsilon \to 0} \frac{\boldsymbol{\xi}(t+T, \mathbf{x}; \varepsilon) - \boldsymbol{\xi}(t, \mathbf{x}; \varepsilon)}{T} \tag{24}$$

$$\text{where} \qquad \boldsymbol{\xi}(T, \mathbf{x}_0, \varepsilon) = \mathbf{x}_0 + \sum_{t_m=1}^{T} (t_m - t_{m-1}) \mathbf{f}(\mathbf{x}(t_m); \varepsilon) \ ,$$

$$\text{and} \qquad \lim_{\varepsilon \to 0} \mathbf{f}(\mathbf{x}; \varepsilon) = \mathbf{f}_i(\mathbf{x}) \quad \text{for } \mathbf{x} \in R_i \ ,$$

for some real $T \geq 0$ and $\varepsilon \geq 0$, time-steps $t_m \in [0, T]$, and initial point $\mathbf{x}_0$, with $\mathbf{f}(\mathbf{x}(t_m); \varepsilon)$ defined such that the limit $\langle \dot{\mathbf{x}} \rangle$ exists.

We then have the discrete-time analogue of definition 3.2.

Definition 3.5. Given a system (23) with indicator function (10), for some $N \in \mathbb{N}$, let $\mathbf{x}(0) = \mathbf{x}_0$, $\mathbf{x}(t_m) = \mathbf{x}_m$, and $\mathbf{x}(T) = \mathbf{x}_N$, we define the *switching multiplier* λ_j, the *mode occupancy* μ_i, and the *switching probability* P_{ki} from

mode k to i, by

$$\lambda_j(N) = \frac{1}{N}\sum_{n=0}^{N} h_j(\mathbf{x}_n) \ , \tag{25}$$

$$\mu_i(N) = \frac{1}{N}\sum_{n=0}^{N} m_i(\mathbf{x}_n) \ , \tag{26}$$

$$P_{ki}(N) = \frac{1}{\mu_k N}\sum_{n=0}^{N} m_k(\mathbf{x}_n) m_i(\mathbf{x}_{n+1}) \ , \tag{27}$$

where $j \in \{1, ..., r\}$ and $k, i \in \{0, ..., d\}$.

The properties in lemma 3.1 and lemma 3.2 apply similarly to these, with proofs that follow analogously, so we omit them here.

Similar to definition 3.3, an augmented form of λ_j, μ_i, and P_{ki}, will be of use for characterising attractors.

Definition 3.6. Given a system (23) with indicator function (10), let $\mathbf{x}(0) = \mathbf{x}_0$ and $\mathbf{x}(t_m) = \mathbf{x}_m$, we define the *asymptotic switching multiplier* $\overline{\lambda}_j$, *asymptotic mode occupancy* $\overline{\mu}_i$, and the *asymptotic switching probability* $\overline{P}_{ki}$ from mode k to i, by

$$\overline{\lambda}_j = \lim_{N\to\infty} \frac{1}{N}\sum_{n=0}^{\infty} (1 - \tfrac{1}{N})^n h_j(\mathbf{x}_n) \ , \tag{28}$$

$$\overline{\mu}_i = \lim_{N\to\infty} \frac{1}{N}\sum_{n=0}^{\infty} (1 - \tfrac{1}{N})^n m_i(\mathbf{x}_n) \ , \tag{29}$$

$$\overline{P}_{ki} = \frac{1}{\mu_k} \lim_{N\to\infty} \frac{1}{N}\sum_{n=0}^{\infty} (1 - \tfrac{1}{N})^n m_k(\mathbf{x}_n) m_i(\mathbf{x}_{n+1}) \ , \tag{30}$$

where $j \in \{1, ..., r\}$ and $k, i \in \{0, ..., d\}$.

3.3 Determinacy of μ-sums

Clearly the mode occupancies μ_i are equal to either 1 or 0 for a trajectory that lies in one mode for all times, and lie between 0 and 1 for trajectories that travel between modes. We also find $\mu_i \in [0, 1]$ for trajectories that travel *along* the boundaries between modes, known as *sliding* along the discontinuity. To find these weighted sums, we consider the following.

Assumption 3.1. Consider a point $\mathbf{x}$ that lies at a point on the boundary of regions R_i, for all $i \in \{0, 1, ..., d\}$ for some d. Assume that in a neighbourhood $U \subset \mathbb{R}^n$ of this point, the boundary of the regions R_i can be expressed as the union of $r < d$ hypersurfaces $\mathcal{D}_j = \{\mathbf{x} \in \mathbb{R}^n \ : \ \sigma_j(\mathbf{x}) = 0\}$, for some smooth functions $\sigma_j : \mathbb{R}^n \to \mathbb{R}$ and $j = 1, ..., r$.

We can then take as coordinates $x_j = \sigma_j$ for $j = 1, ..., r$, and split up $\mathbf{x} = (\mathbf{X}, \mathbf{y})$ with $\mathbf{X} \in \mathbb{R}^r$ and $\mathbf{y} \in \mathbb{R}^{n-r}$, so that $\mathbf{X} = \mathbf{0}$ on the intersection of the hypersurfaces $\mathcal{D}_1 \cap ... \cap \mathcal{D}_r$. Then correspondingly letting $\mathbf{f}_i = (\mathbf{F}_i, \mathbf{g}_i)$, we split the system (1) into its $\mathbf{X}$ and $\mathbf{y}$ parts as

$$\dot{\mathbf{X}} = \mathbf{F}_i(\mathbf{X}, \mathbf{y}) \ , \qquad \dot{\mathbf{y}} = \mathbf{g}_i(\mathbf{X}, \mathbf{y}) \ . \tag{31}$$

If $\mathbf{x}$ lies on the intersection $\mathcal{D}_1 \cap ... \cap \mathcal{D}_r$, and moreover slides along this intersection, then its equivalent dynamics (8) satisfies

$$\langle \mathbf{X} \rangle = 0 \quad \text{and} \quad \langle \dot{\mathbf{X}} \rangle = 0 \qquad \text{for } \ j = 1, ..., r. \tag{32}$$

Henceforth we omit the argument $(\mathbf{X}, \mathbf{y})$ of the functions $\mathbf{F}_i$ or $\mathbf{f}_i$, understanding that all of the expressions below are evaluated at

$$(\mathbf{X}, \mathbf{y}) = (\mathbf{0}, \mathbf{y}) \ . \tag{33}$$

Let us first take the example of $r = 2$ switch indicators from section 2, in which $d = 3$ and $\sigma_j(\mathbf{x}) = x_j$. We will then generalise to the full situation outlined above.

Lemma 3.4 (μ-pair sums)**.** Consider the system (1) with $i \in \{0, 1, 2, 3\}$, under assumption 3.1 and placed in the form (31). Then, during sliding along an intersection of switching thresholds $x_1 = x_2 = 0$, there exist sums of the μ_i coefficients that are fully determined by the conditions (32) with $r = 2$, and given by

$$\begin{pmatrix} \Lambda_1 \\ \Lambda_2 \end{pmatrix} := \begin{pmatrix} \mu_1 \\ \mu_2 \end{pmatrix} + \underline{\underline{A}}^{-1}.(\mathbf{F}_3 - \mathbf{F}_0)\mu_3 = -\underline{\underline{A}}^{-1}.\mathbf{F}_0 \ , \tag{34}$$

provided the 2×2 matrix

$$\underline{\underline{A}} = [\mathbf{F}_1 - \mathbf{F}_0, \mathbf{F}_2 - \mathbf{F}_0] \tag{35}$$

is non-singular.

Proof. Take the conditions (32) with $r = 2$ for sliding motion along the intersection $x_1 = x_2 = 0$. Taking (8) with $d = 3$, use the normalisation condition (9) to eliminate one of the coefficients μ_i. Without loss of generality, if we eliminate μ_0 we obtain

$$\begin{aligned}\langle\dot{\mathbf{X}}\rangle &= (1-\mu_1-\mu_2-\mu_3)\mathbf{F}_0 + \mu_1\mathbf{F}_1 + \mu_2\mathbf{F}_2 + \mu_3\mathbf{F}_3 \\ &= \mathbf{F}_0 + \mu_1(\mathbf{F}_1-\mathbf{F}_0) + \mu_2(\mathbf{F}_2-\mathbf{F}_0) + \mu_3(\mathbf{F}_3-\mathbf{F}_0) \\ &= \mathbf{F}_0 + \underline{\underline{M}}.(\mu_1,\mu_2,\mu_3)^{\mathsf{Tr}}\ , \end{aligned} \tag{36}$$

where $\underline{\underline{M}} = [\mathbf{F}_1-\mathbf{F}_0, \mathbf{F}_2-\mathbf{F}_0, \mathbf{F}_3-\mathbf{F}_0]$, hence a 3×2 matrix. Let us split this into the 2×2 matrix $\underline{\underline{A}} = [\mathbf{F}_1-\mathbf{F}_0, \mathbf{F}_2-\mathbf{F}_0]$, and the vector $\mathbf{F}_3-\mathbf{F}_0$, and assume typically that $\underline{\underline{A}}$ is non-singular. Then $\underline{\underline{A}}$ is invertible, so we can further decompose (36) as

$$\langle\dot{\mathbf{X}}\rangle = \mathbf{F}_0 + \underline{\underline{A}}.(\mu_1,\mu_2)^{\mathsf{Tr}} + (\mathbf{F}_3-\mathbf{F}_0)\mu_3\ . \tag{37}$$

Finally multiplying through by the inverse of $\underline{\underline{A}}$, and applying the sliding condition (32) for $r = 2$, we have in sliding on $\mathbf{X} = 0$ the result (34),

$$(\mu_1,\mu_2)^{\mathsf{Tr}} + \underline{\underline{A}}^{-1}.(\mathbf{F}_3-\mathbf{F}_0)\mu_3 = -\underline{\underline{A}}^{-1}.\mathbf{F}_0\ .$$

□

The implication of these is that, since the μ-pair sums (34) are well-defined, their values will persist under perturbation, unlike the values of the individual μ_is, which are not well-defined, and therefore are dependent on any perturbation (sensitively so, as it turns out). We will verify this numerically using the pilots' scenario from fig. 2 in section 4.

Lemma 3.4 assumes that the matrix $\underline{\underline{A}}$ is non-singular. For a typical set of modes $\mathbf{f}_i$ this will be true. The simplest typical (i.e. non-degenerate) case is that of an affine control system, which takes a particularly simple form (see for example chapter 2 section 4 of [16]), expressible as

$$(\dot{x}_1,\dot{x}_2)^{\mathsf{Tr}} = \mathbf{F}_0 + \underline{\underline{A}}.\,(h_1,h_2)^{\mathsf{Tr}} \tag{38}$$

with $h_j = \mathrm{step}(x_j)$, where $\mathbf{F}_i = \mathbf{F}_0 + \underline{\underline{A}}.\,(h_1,h_2)^{\mathsf{Tr}}$, and $i = h_1 + 2h_2$. Then $\underline{\underline{A}}^{-1}.(\mathbf{F}_3-\mathbf{F}_0) = (1,1)^{\mathsf{Tr}}$, so the quantities Λ_i in (34) become simply the λ_i, that is, the unweighted μ-pair sums

$$\begin{pmatrix}\lambda_1\\ \lambda_2\end{pmatrix} = \begin{pmatrix}\mu_1+\mu_3\\ \mu_2+\mu_3\end{pmatrix} = -\underline{\underline{A}}^{-1}.\mathbf{F}_0\ . \tag{39}$$

So in the case of affine control, these two quantities are well-defined by sliding, however the μ_is individually are not. This is a somewhat counter-intuitive result: the probability that either of the switches h_j are in the '1' position along some trajectory are well-defined, but the combined probability that, say, both are in the '1' position and hence in the mode $i = 3$, is not well-defined. We will expand on this and verify it numerically in section 4.

As a remark on the interpretation of these terms, note that if we express $\mathbf{F}_3 - \mathbf{F}_0$ as a linear combination of the vectors $\mathbf{F}_1 - \mathbf{F}_0$ and $\mathbf{F}_2 - \mathbf{F}_0$, in terms of some real a and b, then we can write this in terms of $\underline{\underline{A}}$ as

$$\mathbf{F}_3 - \mathbf{F}_0 = a(\mathbf{F}_1 - \mathbf{F}_0) + b(\mathbf{F}_2 - \mathbf{F}_0) = \underline{\underline{A}}.\begin{pmatrix} a \\ b \end{pmatrix} ,$$

$$\Rightarrow \qquad \underline{\underline{A}}^{-1}.(\mathbf{F}_3 - \mathbf{F}_0) = \begin{pmatrix} a \\ b \end{pmatrix} . \tag{40}$$

In the case of affine control we have here $a = b = 1$.

Finally, let us generalise lemma 3.4 to multiple switches, following lemma 3.4 almost verbatim.

Theorem 3.1 (μ-r sums)**.** Consider the system (1), under assumption 3.1 and placed in the form (31). Then, during sliding along an intersection of switching thresholds $\mathbf{X} = 0$, there exist sums of the μ_i coefficients that are fully determined by the conditions (32), and given by

$$\mathbf{\Lambda} := \boldsymbol{\mu}_A + \underline{\underline{A}}^{-1}.\underline{\underline{B}}\,\boldsymbol{\mu}_B = -\underline{\underline{A}}^{-1}.\mathbf{F}_0 , \tag{41}$$

where $\boldsymbol{\mu}_{A,B}$ are vectors of the μ_i coefficients,

$$\begin{aligned} \boldsymbol{\mu}_A &= (\mu_{i_1}, ..., \mu_{i_r})^{\mathsf{Tr}} \qquad \text{where all } \; i_k \in L_A , \\ \boldsymbol{\mu}_B &= (\mu_{i_r+1}, ..., \mu_{i_d})^{\mathsf{Tr}} \quad \text{where all } \; i_k \in L_B , \end{aligned} \tag{42}$$

while $\underline{\underline{A}}$ and $\underline{\underline{B}}$ are an $r \times r$ and $r \times (d-r)$ matrix, respectively,

$$\begin{aligned} \underline{\underline{A}} &= [\mathbf{F}_{i_1} - \mathbf{F}_0, ..., \mathbf{F}_{i_r} - \mathbf{F}_0] \qquad \text{where all } \; i_j \in L_A , \\ \underline{\underline{B}} &= [\mathbf{F}_{i_r+1} - \mathbf{F}_0, ..., \mathbf{F}_{i_d} - \mathbf{F}_0] \quad \text{where all } \; i_j \in L_B , \end{aligned} \tag{43}$$

in terms of sets L_A and L_B, containing r and $d - r$ elements respectively, satisfying

$$\begin{aligned} L_A &= \{i_1, ..., i_r\} \subset \{0, 1, ..., d\} \quad s.t. \;\; \det \underline{\underline{A}} \neq 0 , \\ L_B &= \{0, 1, ..., d\} - L_A . \end{aligned} \tag{44}$$

Proof. Take a point where $x_1 = ... = x_r = 0$, and, given assumption 3.1, take coordinates placing the system in the form (31). Then consider the conditions (32) for sliding motion.

Taking (8) with (31), use the condition (9) to eliminate one of the coefficients μ_i. Without loss of generality, if we choose to eliminate μ_0, we obtain

$$\begin{aligned}\langle \dot{\mathbf{X}} \rangle &= (1 - \sum_{i=1}^{d} \mu_i)\mathbf{F}_0 + \sum_{i=1}^{d} \mu_i \mathbf{F}_i \\ &= \mathbf{F}_0 + \sum_{i=1}^{d} \mu_i (\mathbf{F}_i - \mathbf{F}_0) \ . \end{aligned} \tag{45}$$

In matrix form we can write this as

$$\langle \dot{\mathbf{X}} \rangle = \mathbf{F}_0 + \underline{\underline{M}}.(\mu_1, ..., \mu_d)^{\mathsf{Tr}} \ , \tag{46}$$

where $\underline{\underline{M}} = [\mathbf{F}_1 - \mathbf{F}_0, ..., \mathbf{F}_d - \mathbf{F}_0]$ is the $d \times r$ matrix whose rows are the vectors $\mathbf{F}_i - \mathbf{F}_0$ for $i = 1, ..., d$. For $r > 1$, $\underline{\underline{M}}$ is rectangular, and therefore non-invertible.

However, typically we can find some subset of the remaining mode indices, $L_A \subset \{1, .., d\}$, such that the vectors $\mathbf{F}_i - \mathbf{F}_0$ are linearly independent for all $i \in L_A$. Equivalently, L_A can be chosen such that the matrix $\underline{\underline{A}} = [\mathbf{F}_{i_1} - \mathbf{F}_0, ..., \mathbf{F}_{i_r} - \mathbf{F}_0]$ with all $i_k \in L_A$ for $k = 1, ..., r$, has full rank. So, splitting $\underline{\underline{M}}$ into an invertible square $r \times r$ matrix $\underline{\underline{A}}$, and the remaining $r \times (d - r)$ matrix $\underline{\underline{B}}$, that is $\underline{\underline{M}} = [\underline{\underline{A}}, \underline{\underline{B}}]$, we can further decompose (46) as

$$\langle \dot{\mathbf{X}} \rangle = \mathbf{F}_0 + \underline{\underline{A}}.\boldsymbol{\mu}_A + \underline{\underline{B}}.\boldsymbol{\mu}_B \ , \tag{47}$$

where $\boldsymbol{\mu}_A$ and $\boldsymbol{\mu}_B$ are the vectors in (42), and L_A, L_B, satisfy (44). Multiplying through by the inverse of $\underline{\underline{A}}$, and applying the sliding condition (32), we have in sliding on $\mathbf{X} = \mathbf{0}$ the result (41),

$$\boldsymbol{\mu}_A + \underline{\underline{A}}^{-1}.\underline{\underline{B}}.\boldsymbol{\mu}_B = -\underline{\underline{A}}^{-1}.\mathbf{F}_0 \ .$$

□

The key now is that the individual μ_js are not defined by sliding, we know only that they each lie in the interval $\mu_j \in [0, 1]$. However, theorem 3.1 tells us that the weighted sums $\boldsymbol{\mu}_A + \underline{\underline{A}}^{-1}.\underline{\underline{B}}.\boldsymbol{\mu}_B$ do take a well-defined value in sliding, given by $-\underline{\underline{A}}^{-1}.\mathbf{F}_0$.

The pathological case in which such a set L_A cannot be found implies that the vector fields $\mathbf{F}_i$ are too interdependent (hence degenerate), for example if more than $d-r$ of the vectors $\mathbf{F}_i$ are co-linear, and then typically it is not possible to satisfy the sliding conditions (32).

As with two switches, the μ-r sums take their most simple non-degenerate form for an affine control system. These systems are expressible as

$$\dot{\mathbf{X}} = \mathbf{F}_0(\mathbf{X}, \mathbf{y}) + \underline{\underline{A}}(\mathbf{X}, \mathbf{y}).\,(h_1, ..., h_r)^{\mathsf{Tr}} \tag{48}$$

with h_j as given in (11), and where $\underline{\underline{A}}$ is an $r \times r$ matrix. Then $\mathbf{F}_i = \mathbf{F}_0 + \underline{\underline{A}}.\,(h_1, ..., h_r)^{\mathsf{Tr}}$ and we can let $i = \mathcal{B}(h_1, ..., h_r) := h_1 + 2h_2 + ... + 2^{r-1}h_r$, with each $h_j \in \{0, 1\}$, and $\underline{\underline{A}}$ is precisely the matrix given in (43) with $L_A = \left\{ i \in \{0, 1, ..., d\} \ : \ i = 2^{j-1},\ j = 1, ..., r \right\}$. Let $\underline{\underline{A}} = [\mathbf{a}_1, ..., \mathbf{a}_r]$ where $\mathbf{a}_j = \mathbf{F}_{2^{j-1}} - \mathbf{F}_0$, then the columns of $\underline{\underline{B}}$ are all other vectors $(\mathbf{F}_i - \mathbf{F}_0)$ with $i \neq 2^{j-1}$ for any $j = 1, ..., r$. By direct calculation we can then show that the μ-r sums become unweighted, that is, simply sums of 2^{r-1} μ_is,

$$\begin{pmatrix} \sum_{i \in L^1} \mu_i \\ \vdots \\ \sum_{i \in L^r} \mu_i \end{pmatrix} = -\underline{\underline{A}}^{-1}.\mathbf{F}_0 \tag{49}$$

where

$$L^k = \left\{ i \in \{0, 1, ..., d_r\} \ : \ \begin{array}{l} i = i_1 + ... + 2^{r-1} i_r, \\ i_{j \neq k} \in \{0, 1\}\,,\ i_k = 1 \end{array} \right\}. \tag{50}$$

That is, whereas theorem 3.1 gives $\mathbf{f}_i$-weighted sums of the μ_is that are determined by sliding, for a linear switching system these sums are unweighted, and just simple sums of certain μ_is.

3.4 Usage in perturbations

The definitions above are written in such a way that they can be adapted to a wide range of perturbations or simulation methods, where the mode indicator m_i may consist of some set of rules or processes that must be carried out before the system switches to a new mode.

For example, consider perturbations of a simple switch $m(x) = \text{step}(x)$. If it takes a time ε for the switch to a new mode to activate, this may instead take the form $m(x(t)) = \text{step}(x(t - \varepsilon))$. If x is measured by some intermediate variable u, and this triggers the switch, we might have $m(x(t)) =$

step$(u(t))$ with $\varepsilon\dot{u} = x - u$. If the system is smoothed then the indicator might become $m(x) = \phi_\varepsilon(x)$ where ϕ_ε is a differentiable sigmoid function, e.g. $m(x) = \text{sign}(x)/\left(1 + e^{-|x|/\varepsilon}\right)$.

Importantly, this generalises the quantities λ_j, μ_i, and P_{ki}, to perturbations of the idealised system (1), where the modes $\mathbf{f}_i$ no longer apply exactly on distinct regions R_i, but instead may apply on 'fuzzy' or disconnected sets R_i^ε with no distinct boundaries and that might no longer partition space fully. This happens when there is an overshoot of the boundary of a region R_i before a switch occurs, as will be the case in most simulations, or when we smooth a discontinuity. In any such cases it is indistinct where the 'switch' occurs, therefore the concepts of 'switching' or 'mode occupancy' may themselves be indistinct. The integrals in definition 3.2 then provide the definition of these concepts, as integral functions measuring the switching multiplier, mode occupancy, and switching probability. We will put λ_j and μ_i to use in section 4, while the surprising complexity of P_{ki}, even for a single switch, can be seen in its first tentative use [8].

3.5 Uniqueness of the asymptotic mode occupancy

The factor $e^{-t/T}$ in the integrals definition 3.3, and $(1 - N^{-1})^n$ in the sums definition 3.6, ensures that contributions from any transients, say over $t \in [0, T]$ for any finite T, vanish, therefore it is only the asymptote of a trajectory as $t \to \infty$ that determines the values of $\overline{\mu}_i$ and $\overline{P}_{ki}$, ensuring they are associated with a given attractor independent of initial conditions (but there may be more than one co-existing attractor having distinct $\overline{\mu}_i$ and $\overline{P}_{ki}$ values).

Let us illustrate with two very simple examples. The first shows a well-defined equilibrium with a unique asymptotic mode occupancy. The second shows that a degenerate equilibrium may *not* have a unique asymptotic mode occupancy.

Example 3.1 (A stable equilibrium)**.** Consider a trivial discontinuous system $\dot{x} = 1 - 3m_1(x)$ with $m_1(x) = \text{step}(x)$, where the discontinuity at $x = 0$ is an attractor. To calculate $\overline{\mu}_1$ for this attractor, let us consider two different perturbations.

First take Filippov's approach of convex combinations [16], which amount to defining an equivalent dynamics $\langle\dot{x}\rangle = 1 - 3m_1(x)$ with $\mu_1 \in [0, 1]$ at $x = 0$. Although this approach does not explicitly make use of any small ε, we must still consider it to describe the equivalent dynamics of $\langle x\rangle$, not x itself. For any $x_0 < 0$ or $x_0 > 0$, a solution $\langle x(t)\rangle$ reaches $x = 0$ after

time $t = -x_0$ or $x_0/2$, respectively, but because these are finite intervals of time, their contributions to the integrals $\overline{\mu}_1$ vanish, leaving only the motion on $x = 0$ for all later times. For these times, then, we have $\dot{x} = 0$, implying that $m_1(0) = 1/3$. Calculating (14) then gives $\overline{\mu}_1 = 1/3$.

Compare this to the discretisation $x_{n+1} = x_n + (1 - 3\,\mathrm{step}(x))\varepsilon$. For this we use the discrete time form of $\overline{\mu}_1$ from definition 3.5. After some finite q iterations, with $q \in [|x_0|, |x_0| + 1]$ for $x_0 < 0$, and $q \in \left[\frac{1}{2}|x_0|, \frac{1}{2}|x_0| + 1\right]$ for $x_0 > 0$, solutions enter a periodic orbit with two steps in $x < 0$ for every one in $x > 0$, and the calculation in (26) again yields $\overline{\mu}_1 = 1/3$.

Note we have a well-defined value for $\overline{\mu}_1$, whose value is consistent between these (and other) perturbations.

Example 3.2 (A degenerate equilibrium)**.** Now consider a degenerate system $\dot{x} = -x - xm_1(x)$ with $m_1(x) = \mathrm{step}(x)$. Again the point at $x = 0$ is an attractor. The system's solutions are $x(t) = x_0 e^{-t}$ for $x_0 < 0$, $x(t) = x_0 e^{-2t}$ for $x_0 > 0$, and $x(t) = 0$ for $x_0 = 0$.

For initial points $x_0 \neq 0$, we can directly use (14) to calculate $\overline{\mu}_1$. Since these solutions do not cross or touch $x = 0$, only asymptote towards it, we simply have $m_1(x(t)) = m_1(x_0)$, and hence $\overline{\mu}_1 = 1$ if $x_0 > 0$ and $\overline{\mu}_1 = 0$ if $x_0 < 0$. If we use Filippov's approach of convex combinations, assuming $\mu_1(0) \in [0, 1]$, we have $\overline{\mu}_1 \in [0, 1]$ for $x_0 = 0$. Hence $\overline{\mu}_1$ is not unique, taking different values for different initial points x_0.

As in the previous example, we find similar results if we discretise the system as $x_{n+1} = x_n - (1 + \mathrm{step}(x))x_n\varepsilon$, namely that $\overline{\mu}_1 = 1$ if $x_0 > 0$ and $\overline{\mu}_1 = 0$ if $x_0 < 0$. In this case the value for $x_0 = 0$ is indeterminate.

The reason that $\overline{\mu}_1$ is non-unique here is that the attractor is degenerate, consisting of a zero of each field $f_0 = -x$ and $f_1 = -2x$ coinciding with the discontinuity in the derivative at $x = 0$. Under perturbation, say $\dot{x} = -x - xm_1(x) + c$, the equilibrium will typically move to $x = c$ if $c < 0$, giving $\overline{\mu}_1 = 0$, or to $x = c/2$ if $c > 0$, giving $\overline{\mu}_1 = 1$, both well-determined for $c \neq 0$, but undergoing a transition between the two at $c = 0$ where the system undergoes a boundary equilibrium persistence bifurcation.

4 The pilots' dilemma revisited

Let us use the example from section 2 to illustrate some of the results above, focussing here on the implication that, due to the indeterminacy of the μ_is, their values can vary markedly under perturbation, while the determinacy of the μ-pair sums mean their values persist under perturbation.

In fig. 3 we illustrated three variants of the pilot scenario, (i)-(iii). The relevance of these is seen when we write the modes $\mathbf{f}_i$ in terms of switch indicators h_j, as we introduced in (11)-(12). Each pilot $j = 1, 2$, makes a decision h_j depending on whether they find themselves to the negative side (choosing $h_j = 0$) or positive side (choosing $h_j = 1$) of their respective target threshold $x_j = 0$, or simply $h_j = \text{step}(x_j)$. We obtain an expression of the form (12), namely

$$\begin{aligned}\mathbf{f}_i = \mathbf{f}(\mathbf{x}; h_1, h_2) = (1-h_1)(1-h_2)\mathbf{f}_0 + h_1 h_2 \mathbf{f}_3 \\ + h_1(1-h_2)\mathbf{f}_1 + (1-h_1)h_2\mathbf{f}_2 \ , \end{aligned} \tag{51}$$

with the correspondence $i = h_1 + 2h_2$.

The three sets of parameters in fig. 3 then give the particular forms:

$$\begin{aligned} &(i) \qquad (\dot{x}_1, \dot{x}_2, \dot{y}) = (2 - 3h_1 + h_2 - 3h_1h_2, 2 - 3h_2 - 3h_1h_2, 4h_1h_2 - 1), \\ &(ii) \qquad (\dot{x}_1, \dot{x}_2, \dot{y}) = (1 - 3h_1 + h_2, 3 - h_1 - 6h_2, 6h_1h_2 - 1), \\ &(iii) \qquad (\dot{x}_1, \dot{x}_2, \dot{y}) = (3 - 5h_1, 1 - 5h_2, 6h_1h_2 - 1), \end{aligned} \tag{52}$$

their relevance being that their $(\dot{x}_1, \dot{x}_2)$ components have: (i) bi-linear dependence on the h_js, (ii) linear dependence on the h_js, (iii) uncoupled dependence on the h_js (meaning each $\dot{x}_j$ depends only on its respective h_j).

We can now look into why fig. 3 shows such unpredictability in the spaceship's motion between simulations, in each of these variants (i)-(iii), and contrarily, what aspects of the motion *are* well-determined.

For brevity we will choose just one of the simulation methods ①-⑦ from fig. 3, and vary it slightly to illustrate the results from section 3. We will choose variations of method ⑥ for convenience, but similar results can be seen with others. Here, the system evolves in discrete time-steps $\Delta t = 1$, and we will let pilot 2 make decisions every 50 time-steps, while pilot 1 makes decisions every δ time-steps, with $\delta \in [0, 100]$ plotted across the horizontal axis in the figures that follow.

Although time delays of up to 100 steps may seem large, this merely provides a large number of data points for illustration, these time-steps can be taken arbitrarily small and therefore all represent infinitesimal perturbations of the limit (51), not changing as the time-step and delay tend towards zero. Throughout this section we use the appropriate continuous or discrete time form to calculate the μ_i, namely (14) or (26), and integrate over sufficiently long times that they settle to steady values, approximating the value $\mu_i \approx \overline{\mu}_i$ of the attractor that they fall onto around the steady state $x_1 = x_2 = 0$.

4.1 μ-pair sums, and μ_i indeterminacy

In fig. 4 we take the 3 variants (i)-(iii) from fig. 3, and numerically calculate the μ-pair sums from the left-hand side of (34) in (i) or (39) in (ii)-(iii) (blue lines), showing they indeed line up with their predicted values on the right-hand side of (34) (red dotted lines). The individual μ_is vary, however, as we vary parameters of the simulation, and here we plot just μ_3 (black curve) as an example. Remember that in each graph, the system itself is not changing with δ, only the response-time of the first pilot.

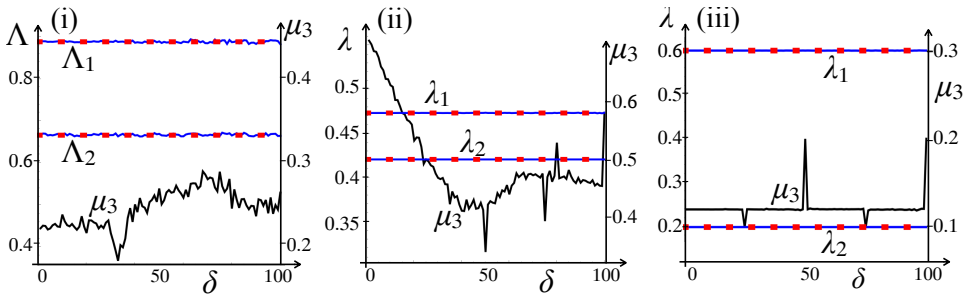

Figure 4: Numerical μ_3 (black), numerical μ-pair sums (Λ_1, Λ_2) from (34) (blue), exact $-\underline{\underline{A}}^{-1}.\mathbf{f}_0$ from (34) (red dotted). Simulated in discrete time-steps $\Delta t = 1$, with pilot $\{x_1, x_2\}$ making decisions every $\{\delta, 50\}$ steps. Simulations run for 10^5 time-steps. (i)-(iii) correspond to those in fig. 3. In (ii)-(iii) we have $(\Lambda_1, \Lambda_2) := (\lambda_1, \lambda_2)$ by (39).

The variability in μ_3 (and in the other μ_i's not shown) then explains the variability seen in fig. 3. Infinitesimal changes in the simulation – here in the first pilot's response time δ – change the probability that they system is in any of its given modes as indicated by the μ_is, and hence change the resulting forward motion as we simulated in fig. 3. The spaceship's instantaneous forward motion in these simulations has the form $\dot{y} = -\gamma_0 + \gamma_3 h_1 h_2$, but its equivalent dynamics is $\langle \dot{y} \rangle = -\gamma_0 + \gamma_3 \mu_3$, so the unpredictability of μ_3 translates into unpredictability of $\langle \dot{y} \rangle$.

For different parameters and different simulations methods, the amount of variation in the μ_is can vary significantly. In the case where the two pilots act entirely independently, in (iii), we see that μ_3 is almost constant, and yet it has spikes in value around $\delta = 25, 50, 75$. This is surprising because λ_1 and λ_2 give the probabilities that pilots 1 and 2 make decisions $h_1 = 1$ and $h_2 = 1$, respectively, and μ_3 represents the probability that both pilots decide $h_j = 1$. In (i) it might be unclear whether the pilots' decisions are dependent, in (ii) their decisions are *taken* independently but may have co-dependent action on the system, but in (iii) their decisions and their effect

on the x_1-x_2 system are entirely independent, yet the spike in fig. 4 reveal that, nevertheless, a dependence emerges over time.

This dependence is associated with the geometry of the system's attractor near the intersection $x_1 = x_2 = 0$. In fig. 5 we show the attractor near two of the spikes in μ_3 in fig. 4(iii), with the resulting change in the value of μ_3.

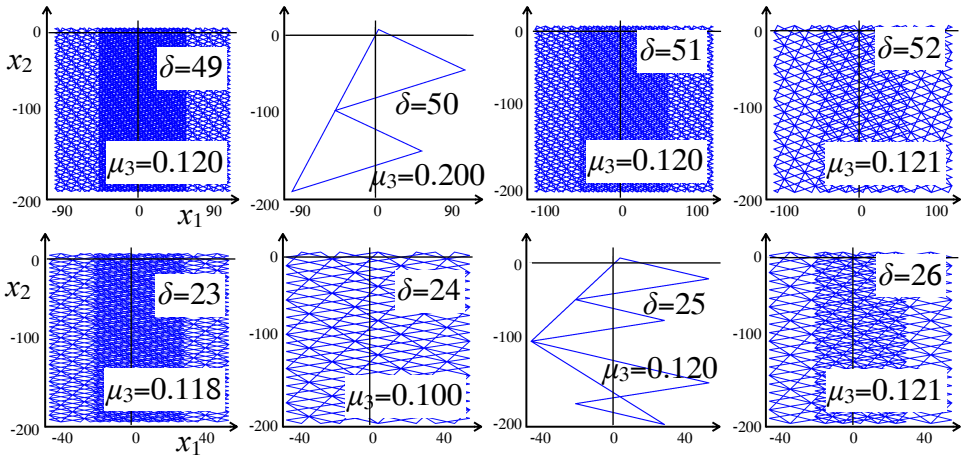

Figure 5: Attractors of the system from fig. 4(iii), showing that the attractor and the value of μ_3 are similar at $\delta = 49, 51, 52$, and again at $\delta = 23, 24, 26$, while the spike in μ_3 seen in fig. 4(iii) at $\delta = 50$ and 25 accompanies a significant change in the attractor. (Initial condition $x_1(0) = 2.5$, $x_2(0) = 2.5$. Each simulation is run for $t = 10^5$ time-steps.

Relations between the attractor geometry and the variation in the μ_is have been observed before. It was shown numerically for various perturbations in [20], shown rigorously for hysteresis across the switching thresholds in [1, 22] or for a discrete and delayed time system across a single switching threshold in [8]. The analysis of such perturbations is intractably hard to generalise. For the first time, with rigorous definitions of μ_i, P_{ki}, and λ_j, we can generalise this to any kind of system without such detailed prescription of the perturbation.

It should be noted typically in such systems that these attractors need not be unique, and hence even if $\overline{\mu}_i$ is unique for a given attractor by **??**, multiple values of $\overline{\mu}_i$ may still be possible in the region of a point like $x_1 = x_2 = 0$ in the pilots' scenario, depending on initial condition. In fig. 6, for the same system with a simple forward Euler discretisation with time-step $\Delta t = 1$, and with both pilots making decisions every 50 time-steps, we plot

four distinct attractor shapes found with different initial conditions, along with their associated μ_3 values. Recall that the size of this time-step is arbitrary, so this is equivalent to simply taking a time-step $\Delta t = 50$, which again can be taken arbitrarily small without changing the results shown (hence e.g. the same plots are found with $\Delta t = 1$ up to re-scaling).

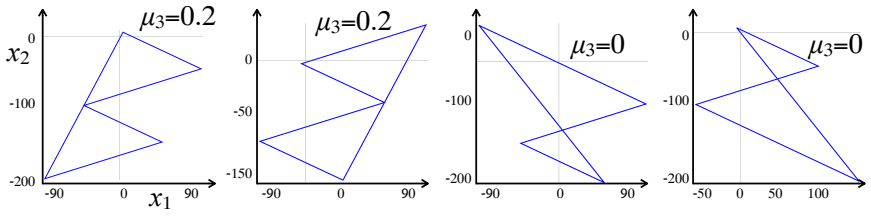

Figure 6: Attractors of the system from fig. 5 but with both pilots making decisions at each time-step, showing three different attractors obtained with the same parameters but different initial conditions $(x_1, x_2) = (\pm 2.5, \pm 2.5)$. (In the first two panels $\mu_2 = 0$).

4.2 Smoothing as a special case

In section 1 we discussed whether the decisions of the pilots could be treated as independent in a probabilistic sense. We can express the condition (6) now in terms of the probabilities μ_i and λ_i, that if the two pilots behave independently, we would expect that

$$\mu_3 = \lambda_1 \lambda_2 \ .$$

Here we can show that this does not hold in general.

We shall start with the one special case where these conditions strictly hold upon simulation, and that is if we smooth out the discontinuity. To see this, let us look at what happens when we smooth (51). This is done (e.g. using the influential Sotomayor-Teixeira regularisation [34]) by replacing each step function h_j in the expression (51) with a smooth monotonic function H_j^ε that satisfies $h_j(\mathbf{x}) = \lim_{\varepsilon \to 0} H_j^\varepsilon(\mathbf{x})$, giving

$$\begin{aligned} \dot{x} = &(1 - H_1^\varepsilon)(1 - H_2^\varepsilon)\mathbf{f}_0 + H_1^\varepsilon H_2^\varepsilon \mathbf{f}_3 \\ &+ H_1^\varepsilon (1 - H_2^\varepsilon)\mathbf{f}_1 + (1 - H_1^\varepsilon) H_2^\varepsilon \mathbf{f}_2 \ , \end{aligned} \tag{53}$$

In simulations here we use $H_j^\varepsilon(\mathbf{x}) = \frac{1}{2}\left(1 + \tanh(x_j/\varepsilon)\right)$.

Now let us write down the equivalent dynamics. First, the general form from (8) is

$$\langle \dot{\mathbf{x}} \rangle = \mu_0 \mathbf{f}_0 + \mu_1 \mathbf{f}_1 + \mu_2 \mathbf{f}_2 + \mu_3 \mathbf{f}_3 \ . \tag{54}$$

If the μ_is and λ_js behave like independent probabilities, that is with μ_i being the probability the system is in the mode with $m_i = 1$, and λ_j being the probability the system is in any mode with $h_j > 0$, then if we can combine these as unconditional probabilities we have

$$\begin{aligned} \mu_0 &= (1-\lambda_1)(1-\lambda_2)\ , & \mu_1 &= \lambda_1(1-\lambda_2)\ , \\ \mu_2 &= (1-\lambda_1)\lambda_2\ , & \mu_3 &= \lambda_1\lambda_2\ . \end{aligned} \tag{55}$$

Substituting these into (54) gives

$$\begin{aligned} \langle\dot{\mathbf{x}}\rangle = (1-\lambda_1)(1-\lambda_2)\mathbf{f}_0 + \lambda_1\lambda_2\mathbf{f}_3 \\ + \lambda_1(1-\lambda_2)\mathbf{f}_1 + (1-\lambda_1)\lambda_2\mathbf{f}_2\ , \end{aligned} \tag{56}$$

i.e. just the expression (51) with the h_js replaced by the λ_js. This makes sense for a smooth system, since the same equations hold for all time, and is proven in [34]; this is also easily verified by simulation as we will do in fig. 7 below.

If other perturbations are closely approximated by smoothing, then (55) should hold at least approximately, but we shall see it does not. We will first show this using the simulations from fig. 4, and then give a particular geometrical counterexample.

Figure 7 shows, for the simulations from fig. 4, the value of $\lambda_1\lambda_2$ (blue curve), calculated using lemma 3.4 for $j = 1, 2$. We also plot μ_3 (black curve) repeated from fig. 4. Lastly we plot $\lambda_1\lambda_2$ calculated for a smoothed system (blue dotted, the smoothing functions are not important, but here we use $H_j^\varepsilon(u) = \frac{1}{2}(1 + \tanh(u/\varepsilon))$).

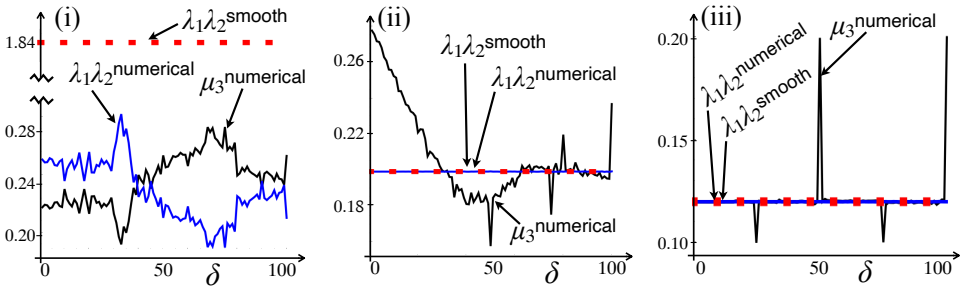

Figure 7: The values of $\lambda_1\lambda_2$ (blue curve) and μ_3 in the simulations from fig. 4, and the values of $\lambda_1\lambda_2$ simulated from a smoothed system (blue dotted).

In (i), the only well-determined quantities are the μ-pair sums (34), so the direct sums $\lambda_j = \mu_j + \mu_3$ are not well-determined, hence $\lambda_1\lambda_2$ is not

well-determined, and we see how its value then differs between the discrete numerical and smoothed simulations. Moreover, these differ from μ_3, that is, $\lambda_1\lambda_2 \neq \mu_3$, and $\lambda_1\lambda_2$ itself is not even well-determined, so (55) does not hold.

In (ii)-(iii), because these systems have linear dependence on the h_j, these are an affine system and satisfy (39), so the $\lambda_j = \mu_j + \mu_3$ are well-determined, hence the products $\lambda_1\lambda_2$ are well-determined. This makes the value of $\lambda_1\lambda_2$ stable to perturbation, hence its value agrees between the discrete numerical and smoothed simulations. Nevertheless, again these differ from μ_3 in general. Even in the uncoupled case (iii), when each pilot acts entirely separately of the other, the relation $\lambda_1\lambda_2 \approx \mu_3$ holds for some but not all values of the delay δ, in this case precisely failing at the spikes around $\delta = 25, 50, 75$.

We can also construct particular counterexamples that show that the relations (55) will not hold in general, similar to the attractors in fig. 6.

Consider an attractor formed by only three modes, so that one of the μ_i vanishes. Then it is a trivial result that $\mu_3 \neq \lambda_1\lambda_2$, contrary to (55), therefore such a system will not behave like the smoothed system (where $\mu_3 = \lambda_1\lambda_2$). To see this, without loss of generality, say the attractor is made up of the modes $i = 0, 1, 2$, therefore λ_1 and λ_2 are nonzero (meaning the attractor spends time in both $x_1 > 0$ and $x_2 > 0$), but $\mu_3 = 0$ (meaning the occupancy time in $\{x_1 > 0 \ \wedge \ x_2 > 0\}$ is zero), therefore clearly $\mu_3 \neq \lambda_1\lambda_2$ Now let us show that such an attractor can exist in general.

Look for an attractor formed by any 3 modes. Let $L_k = \{0, 1, 2, 3\} - \{k\}$ for $k = 0, 1, 2, 3$. From (36), an attractor of the sliding system on $x_1 = x_2 = 0$, comprised only of the modes in L_k such that $\mu_k = 0$, has equivalent dynamics satisfying

$$\begin{aligned} 0 &= \mathbf{F}_r + \mu_p(\mathbf{F}_p - \mathbf{F}_r) + \mu_q(\mathbf{F}_q - \mathbf{F}_r) \\ &= \mathbf{F}_r + [\mathbf{F}_p - \mathbf{F}_r, \mathbf{F}_q - \mathbf{F}_r] \, .(\mu_p, \mu_q)^{\mathsf{Tr}} \\ \Rightarrow \quad \begin{pmatrix} \mu_p \\ \mu_q \end{pmatrix} &= -\underline{\underline{A}}^{-1}.\mathbf{F}_r \quad \text{and} \quad \mu_r = 1 - \mu_p - \mu_q \ , \end{aligned} \tag{57}$$

where p, q, r, are distinct integers in L_j, with $\underline{\underline{A}} = [\mathbf{F}_p - \mathbf{F}_r, \mathbf{F}_q - \mathbf{F}_r]$. Since we can choose k to be any one of the four indices, this implies that there may be up to four different attractors of this form, with different shapes, and different μ_i values (clearly these are different since for each choice of k, a different one of the μ_is is zero).

Depending on the method of simulation, these attractors may or may not exist. We can show that these conditions can typically be satisfied in a

system with fixed discrete time-steps. Let $\mu_i = \frac{n_i}{N}$, $n_i \in \{0, ..., N\}$. Then from (57) we have

$$\begin{aligned}\begin{pmatrix} n_p \\ n_q \end{pmatrix} &= -N\underline{\underline{A}}^{-1}.\mathbf{F}_r \quad \text{and} \quad n_r = N - n_p - n_q \ , \\ &= -\tfrac{N}{m_{p1}m_{q2}-m_{p2}m_{q1}} \begin{pmatrix} m_{q2} & -m_{p2} \\ -m_{q1} & m_{p1} \end{pmatrix} . \begin{pmatrix} m_{r1}m_{r2} \end{pmatrix} \\ &:= \begin{pmatrix} a_1/b_1 \\ a_2/b_2 \end{pmatrix} N \end{aligned} \tag{58}$$

where $a_j, b_j \in \mathbb{Z}$, assuming the components of the $\mathbf{F}_i$ are rational. If we assume the attractor is traversed once in S time-steps, and consider a trajectory that travels round it b_1b_2 times, for which $N = b_1b_2S$. Then $(n_p, n_q) = (a_1b_2, b_1a_2)$. It is just such attractors that we see in the pilot scenario in fig. 6, responsible for the spikes in the value of μ_3 where $\mu_2 = 0$, and for two alternative attractors with $\mu_3 = 0$.

5 Closing remarks

When a discontinuity occurs in a dynamical system, its solutions are necessarily non-unique, as different manners of handling the discontinuity may result in qualitatively different solutions. What, then, determines what those solutions look like in a physical system being modelled, or in a simulation of the system? If discontinuities in a dynamical system represent independent decisions, do they behave like independent events over intervals of time, and are they at all determined by the structure of the system of equations?

Within specific applications there have been varied considerations of this problem. The paper [14], for instance, highlights that assumptions are needed beyond Filippov's theory (from [16]) to guarantee uniqueness of solutions in economic models, while [24] investigates how bifurcations are affected by replacing impact discontinuities with elastic contact. But in the great landscape of behaviours that nonsmooth systems are supposed to approximate, it is unclear generally both how solutions $\mathbf{x}(t)$ depend on the method by which they are obtained, (e.g. by analytical or numerical methods), or conversely, whether such a discontinuous model approximates the behaviour of any of the systems like those in fig. 1 that it is intended to. Attempting to answer these questions by somehow 'regularising' the discontinuity leads to tautologies – the solutions obtained depend on the manner of regularisation chosen – but as we we have shown here, more clarity is obtained by strictly distinguishing between an idealised model in the form

(1), and the 'equivalent' dynamics of any system that tends to (1) in some limit.

Using this idea, we have shown here that there are more restrictions on solutions than previously known, through the μ sums, which are weighted by the system's modes in general, or unweighted if the system is of affine/linear form. Therefore, multiple discontinuities, determined by independent processes, *cannot* be treated as independent events probabilistically. Rather, a system will evolve onto an attractor whose form depends sensitively on the fine mechanics of the discontinuity, whether in the modelled or simulated system. That attractor defines the probabilities of occupancy in, and switching between, the system's modes.

In terms of the pilots' scenario we can describe this as follows. Say, after some time T, pilots 1 and 2 are observed to fire their thrusters in the negative ($h_j = 1$) direction $\frac{3}{5}$ and $\frac{1}{5}$ of the time, respectively. Does this suggest that the probability they will be found both firing their thrusters as such at some time is $\frac{3}{5} \times \frac{1}{5} = \frac{3}{25}$, like the flipping of a pair of independent (but biased) coins? In the scenario of fig. 3(iii), we have exactly these individual probabilities, namely $\lambda_1 = \frac{3}{5}$ and $\lambda_2 = \frac{1}{5}$, confirmed in the simulations in fig. 4(iii). The same figure shows that the combined probability, μ_3, is indeed $\frac{3}{25} = 0.12$ for *most* values of δ (the arbitrarily small different in the pilots' reaction times), but not *always*. Attractors can be formed – those shown in fig. 6 – that create spikes in the probability μ_3 (and similarly in the other mode probabilities μ_0, μ_1, μ_2, though we have not plotted them), and these are dependent on the method of simulation, not the logical make-up of the system in the constitutive laws (52). Interestingly, the places where these probabilistic expectations are violated are not obscure, rather the largest deviation occurs where the pilots' decisions are synchronised.

This means the intuitive logic of a discontinuous model is not guaranteed to hold dynamically (and in fig. 4(i-ii) it holds even less so), it is subject to the dynamics that emerges and the method by which the model's solutions are obtained: the *perturbation* of the discontinuous model as we have described it here. The breakdown in logical structure can manifest itself in real system behaviour, in this case the unpredictability of the spaceship's forward motion dependent on simulation method in fig. 3, despite it being essentially an incredibly simple two-player game.

This does not imply that all systems with decisions, switches, controls, or other discontinuous parameters, will behave so unpredictably, only that they *may* do so, and that there is no mathematical justification for expecting that they will not. The pilots' dilemma of section 2 from [21] was conceived to expose precisely the situation where such behaviour would show most

clearly, when a system crosses one or more switching thresholds, repeatedly.

The determinacy of the μs and their sums gives insight into how a discontinuous system behaves under perturbation. The intuition is that quantities that are well-defined perturb regularly, like the weighted μ-sums Λ, or the unweighted sums equal to the switch identifiers λ_j in an affine control system. Quantities that are not well-defined perturb singularly, being dependent on the form of perturbation, and therefore varying between different simulations. This intuition is confirmed in fig. 4 and fig. 7, and is the cause of the uncertainty seen in fig. 3. Whether the dependence on the h_js is linear or nonlinear in the x_j variables, the mode occupancies μ_i vary between simulations.

The fact that such unpredictability occurs at discontinuities can be seen as a consequence of the Picard–Lindelöf existence and uniqueness theorem failing to hold at a discontinuity, though this is often overlooked. The seminal book by Filippov [16] proved the existence of solutions at discontinuities, and gave a convention for obtaining one particular type of solution, often called a *Filippov system*, but this does not remove the inherent non-uniqueness, and we have shown here in fig. 3 how this can affect the reliability of simulations. Hence we propose that it is important to distinguish between the idealised model that satisfies (1), but is ill-defined at the discontinuities, and any method to extend that definition across the discontinuities, which should be considered as belonging to the equivalent dynamics (4). This equivalent dynamics extends the concept of *equivalent control* due to Utkin [38, 33, 23]), making it both more precise and more general, and importantly, defining it in a manner that describes what happens when we perturb away from the limit (1), and it is in this direction that we hope our work will help the study of nonsmooth dynamics progress.

A The simulation methods in fig. 3

The simulation methods in fig. 3 are as follows:

① discrete: the system (51) is simulated in discrete time-steps $\Delta t = \varepsilon$ as $\mathbf{x}_{n+1} = \mathbf{x}_n + \Delta t \mathbf{f}_i(\mathbf{x}_n)$; these simulations take $\varepsilon = 1$.

② smoothed: the system (51) is first smoothed by replacing the steps functions with sigmoids, as $h_j \to \frac{1}{2}\left(1 + \tanh(x_j/\varepsilon')\right)$, taking $\varepsilon' = 0.1$.

③ smoothed in discrete time: the system is smoothed as in ②, then discretised similar to ①, with sigmoid parameter $\varepsilon' = 2$ and time-step $\varepsilon = 1$.

④ shallower sigmoid in discrete time: similar to ④ but with a shorter time-step, $\varepsilon' = \varepsilon = 1$.

⑤ intermediary variable: an intermediary variable facilitates switching by replacing h_j with

$$h_j \to \text{step}(z_j) \ , \qquad \varepsilon' \dot{z}_j = x_j - z_j \ ,$$

and then discretised with time-step $\Delta t = 1$; this simulation takes $\varepsilon' = 3$ and $\varepsilon = 1$.

⑥ delay: simulating delay in the pilots' decisions, the system is discretised as in ①, then the value of h_j is updated only every 2 time-steps for pilot x_1 and every 3 time-steps for pilot x_2.

⑦ random delay: similar to ⑥, except each time x_j changes sign the respective pilot waits a time $\Delta t = \varepsilon$random # in (0,15) before switching the value of h_j.

Each can be considered a *regularisation* or *perturbation* of the ideal system (51).

References

[1] J. C. Alexander and T. I. Seidman. Sliding modes in intersecting switching surfaces, II: Hysteresis. *Houston J. Math*, 25(1):185–211, 1999.

[2] J. A. Amador, J. M. Redondo, G. Olivar-Tost, and C. Erazo. Cooperation-based modeling of sustainable development: An approach from Filippov's systems. *Complexity*, 1(4249106), 2021.

[3] V. Avrutin, L. von Schwerin-Blume, R. Zhusubaliyev, Z.T. an Haroun, and A. El Aroudi. Noise-induced and border-collision-induced bubbling. *Physica D: Nonlinear Phenomena*, 435:133277, 2022.

[4] A. Baule, H. Touchette, and E. G. D. Cohen. Stick–slip motion of solids with dry friction subject to random vibrations and an external field. *Nonlinearity*, 24:351–372, 2011.

[5] J. Bhattacharyya, M. Banerjee, and S. Banerjee. Non-smooth dynamics of a fishery model with a two-threshold harvesting policy. *Communications in Nonlinear Science and Numerical Simulation*, 133:107980, 2024.

[6] C. Budd and R. Kuske. Dynamic tipping and cyclic folds, in a one-dimensional non-smooth dynamical system linked to climate models. *Physica D: Nonlinear Phenomena*, 457:133949, 2024.

[7] T. Carvalho, D. D. Novaes, and D. J. Tonon. Sliding motion on tangential sets of Filippov system. *preprint https://arxiv.org/abs/2111.12377*, 2021.

[8] S. Catsis, C. L. Hall, and M. R. Jeffrey. The hidden sensitivity of nonsmooth dynamics. *Physica D: Nonlinear Phenomena*, 463(134165):1–13, 2024.

[9] A.R. Champneys and P.L. Várkonyi. The Painlevé paradox in contact mechanics. *IMA Journal of Applied Mathematics*, 81(3):538–588, 07 2016.

[10] D. Chieregato Vicentin, P.F.A. Mancera, T. Carvalho, and L. Fernando Gonçalves. Mathematical model of an antiretroviral therapy to hiv via filippov theory. *Applied Mathematics and Computation*, 387:125179, 2020. Computational and Industrial Mathematics.

[11] A. Choudhary, A. Radhakrishnan, J. F. Lindner, S. Sinha, and W. L. Ditto. Neuronal diversity can improve machine learning for physics and beyond. *Scientific Reports*, 13(1):13962, 2023.

[12] S. Coombes, M. Sayli, R. Thul, M.A. Nicks, R .and Porter, and Y.M Lai. Oscillatory networks: Insights from piecewise-linear modeling. *arXiv.2308.09655*, 2023.

[13] R. Coutinho, B. Fernandez, R. Lima, and A. Meyroneinc. Discrete time piecewise affine models of genetic regulatory networks. *Journal of Mathematical Biology*, 52:524–70, 2006.

[14] B. Eckwert and U. Schittko. Disequilibrium dynamics. *The Scandinavian Journal of Economics*, 90(2):189–209, 1988.

[15] R. Edwards, A. Machina, G. McGregor, and P. van den Driessche. A modelling framework for gene regulatory networks including transcription and translation. *Bull. Math. Biol.*, 77:953–983, 2015.

[16] A. F. Filippov. *Differential Equations with Discontinuous Righthand Sides*. Kluwer Academic Publ. Dortrecht, 1988 (original in Russian 1985).

[17] I. Flügge-Lotz. *Discontinuous Automatic Control*. Princeton University Press, 1953.

[18] T. Ito. A Filippov solution of a system of differential equations with discontinuous right-hand sides. *Economics Letters*, 4:349–354, 1979.

[19] M. R. Jeffrey. *Hidden Dynamics: The mathematics of switches, decisions, & other discontinuous behaviour*. Springer, 2019.

[20] M. R. Jeffrey. *Modeling with nonsmooth dynamics*. Frontiers in Applied Dynamical Systems. Springer Nature Switzerland, 2020.

[21] M. R. Jeffrey. Uncertainty in classical systems (with a local, non-stochastic, nonchaotic origin). *J. Phys. A*, 53(115701):1–15, 2020.

[22] M. R. Jeffrey, G. Kafanas, and D. J. W. Simpson. Jitter in dynamical systems with intersecting discontinuity surfaces. *IJBC*, 28(6):1–22, 2018.

[23] M. R. Jeffrey, T. I. Seidman, M. A. Teixeira, and V. I. Utkin. Into higher dimensions for nonsmooth dynamical systems. *Physica D*, 434(133222):1–13, 2022.

[24] H. Jiang, A. S. E. Chong, Y. Ueda, and M. Wiercigroch. Grazing-induced bifurcations in impact oscillators with elastic and rigid constraints. *International Journal of Mechanical Sciences*, 127:204–14, 2017.

[25] Yu. A. Kuznetsov, S. Rinaldi, and A. Gragnani. One-parameter bifurcations in planar Filippov systems. *Int. J. Bif. Chaos*, 13:2157–2188, 2003.

[26] G. F. Lawler. *Introduction to Stochastic Processes.* (2nd ed.). CRC Press, 2006.

[27] J. Leifeld. Non-smooth homoclinic bifurcation in a conceptual climate model. *Euro. Jnl of Applied Mathematics, Special Issue 5 (Theory and applications of nonsmooth dynamical systems)*, 29:891–904, 2018.

[28] A. Machina, R. Edwards, and P. van den Dreissche. Singular dynamics in gene network models. *SIAM J. Appl. Dynam. Sys.*, 12(1):95–125, 2013.

[29] A. A. Markov. Extension of the limit theorems of probability theory to a sum of variables connected in a chain. *The Notes of the Imperial Academy of Sciences of St. Petersburg VIII Series, Physio-Mathematical College*, XXII/9, 1907.

[30] S. H. Piltz, M. A. Porter, and P. K. Maini. Prey switching with a linear preference trade-off. *SIAM J. Appl. Math.*, 13(2):658–682, 2014.

[31] A. Ponosov, I. Shlykova, and R. I. Kadiev. Effects of small random perturbations in the extended glass–kauffman model of gene regulatory networks. *Mathematics*, 12(8), 2024.

[32] S. W. Shaw. On the dynamics response of a system with dry friction. *J. Sound Vib.*, 108(2):305–325, 1986.

[33] J. Shi, J. Guldner, and V. I. Utkin. *Sliding mode control in electro-mechanical systems.* CRC Press, 1999.

[34] J. Sotomayor and M. A. Teixeira. Regularization of discontinuous vector fields. *Proceedings of the International Conference on Differential Equations, Lisboa*, pages 207–223, 1996.

[35] H. Stommel. Thermohaline convection with two stable regimes of flow. *Tellus*, 13:224–230, 1961.

[36] I. Sushko and F. Tramontana. Regular and chaotic dynamics in a 2d discontinuous financial market model with heterogeneous traders. *Mathematics and Computers in Simulation*, 2024.

[37] B. Tang, Y. Xiao, and J. Wu. A piecewise model of virus-immune system with two thresholds. *Mathematical Biosciences*, 278:63–76, 2016.

[38] V. I. Utkin. *Sliding modes and their application in variable structure systems*, volume (Translated from the Russian). MiR, 1978.

[39] V. I. Utkin. Comments for the continuation method by A.F. Filippov for discontinuous systems, part i-ii. *Trends in Mathematics: Research Perspectives CRM Barcelona (Birkhauser)*, 8:177–188, 2017.

[40] J. Valencia-Calvo, G. Olivar-Tost, J. D. Morcillo-Bastidas, C. J. Franco-Cardona, and I. Dyner. Non-smooth dynamics in energy market models: A complex approximation from system dynamics and dynamical systems approach. *IEEE Access*, 8:128877–128896, 2020.

[41] Z.T. Zhusubaliyev, V. Avrutin, A.S. Kucherov, R. Haroun, and A. El Aroudi. Period adding with symmetry breaking/recovering in a power inverter with hysteresis control. *Physica D: Nonlinear Phenomena*, 444:133600, 2023.